Finite Element Analysis of Casing and Casing Connections for Shale Gas Wells

Jueren Xie

C-FER Technologies, Canada

***Abstract**: The application of horizontal drilling and hydraulic fracturing has enabled operators to rapidly develop shale gas production from deep shale formations over the past decade. It has, however, presented significant challenges to casing and casing connection designs due to the complicated and extreme load conditions within these wells. Advanced Finite Element Analysis (FEA) is therefore required to understand casing deformation mechanisms and to assist well designs. This paper presents FEA models developed using Abaqus for analyzing casing and casing connections under shale gas well load scenarios, such as horizontal well installation, perforating and hydraulic fracturing pressures, and formation shear movement. Analysis examples are provided.*

***Keywords**: Bending, Buckling, Casing, Connections, Constitutive Model, Damage, Deformation, Design Optimization, Drilling, Dynamics, Explosive, Failure, Fatigue, Formation Shear, Fracture, Geomechanics, Hydraulic Fracture, Optimization, Perforation, Plasticity, Seal, Soils, Soil-Structure Interaction, Structural Integrity, Wellbore, and Well Installation.*

1. Introduction

Shale gas is an unconventional resource which requires an enhanced extraction method to facilitate its production from low permeable rocks. Over the past decade, the application of horizontal drilling and hydraulic fracturing has enabled operators to rapidly develop shale gas production from deep shale formations. Figure 1 shows a schematic representation of a horizontal shale gas well undergoing hydraulic fracturing.

The use of horizontal drilling and hydraulic fracturing has, however, presented significant challenges to well completion designs. One of the key failure modes for a well is leakage. When leakage occurs, the well function of isolating gases from the aquifer layers can be compromised. Nikiforuk (2013) noted that 5% to 7% of all new oil and gas wells leak, and as wells age the percentage of wells which leak can increase to a startling 30% to 50%. Wittmeyer (2013) suggested that the high casing pressure from fracturing operations and the lack of a pressure relief system are the primary failure modes for shale gas wells. Ghassemi (2011) pointed out that shale stimulation causes a combination of tensile and shear failure. This can occur as shear slippage is induced by the intense stresses near the tip of the fractures, as well as by the increased pore pressure in response to leak-off. Casing failure due to formation shear movement is also considered one of the key failure modes in shale gas wells.

Due to the complicated and extreme load conditions in installation, stimulation and production, casing and casing connection designs for shale gas wells require the use of advanced FEA models. This paper presents FEA models developed using Abaqus for analyzing casing and casing connections under shale gas well load scenarios, such as horizontal well installation, perforating and hydraulic fracturing pressures, and formation shear movement. Analysis examples are provided.

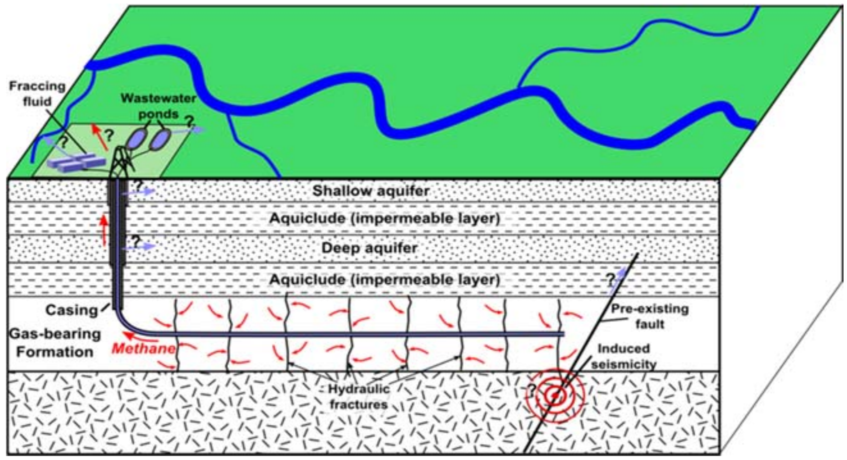

http://en.wikipedia.org/wiki/File:HydroFrac.pen

Figure 1. Schematic depiction of hydraulic fracturing for shale gas.

2. Well Completion Design Considerations

Figure 2 shows a schematic representation of a horizontal well construction. Wellbore construction typically includes conductor casing, surface casing, intermediate casing and production casing. Casing designs are defined by size (i.e. OD), weight, grade (i.e. material strength), and connections. Premium connections are typically used to join casing strings (e.g. 13 m long) in shale gas wells. The horizontal portion of the well is often perforated. The perforation is defined by the perforation hole size, hole density, and phase angle.

Casing connection is a critical element in well completion design. Payne and Schwind (1999) noted that, based on industry estimates, connection failures account for 85% to 95% of all oilfield tubular failures. Connection failures can include structural failure and/or leakage. In the FEA models, the structural failures are defined as parting and/or fatigues at critical locations such as the thread roots, coupling groove and shoulder (see Figure 3). The connection sealing capacity is described by the contact stress profile in the seal region. Various design criteria have been established for assessing connection structural and sealing performance (Xie et al. 2011, and Xie 2013).

Casing and casing connection designs for shale gas wells should consider the following load scenarios:

- Phase 1 – Installation:
  impact of well depth and build angle on casing structural integrity
- Phase 2 – Stimulation:
  impact of perforating and fracturing pressure on casing structural integrity
- Phase 3 – Operation:
  impact of formation shear movement on casing connection structural and sealing integrities

The following sections present FEA models for analyzing casing and casing connections under the above load scenarios. Analysis examples presented in this paper consider a 7 inch, 23 lb/ft L80 casing and connection, with L80 material which is modeled using elastic-plastic constitutive relationships, a Young's modulus of 30,000 ksi, and yield strength of 80 ksi.

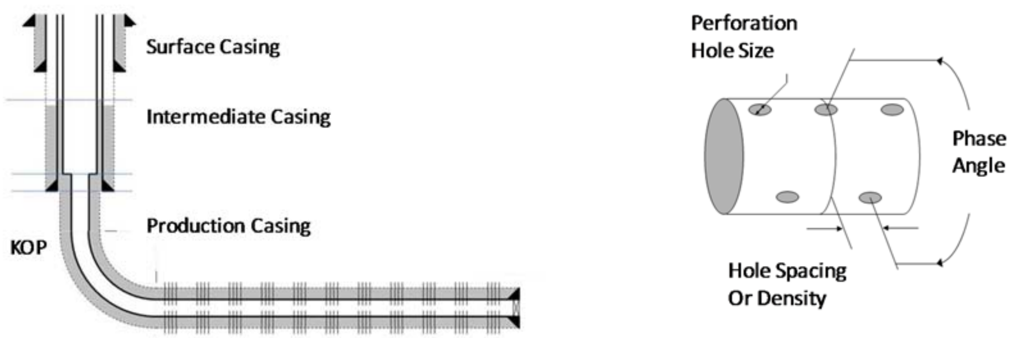

Figure 2. Schematic depiction of well completion design (left) and perforation (right).

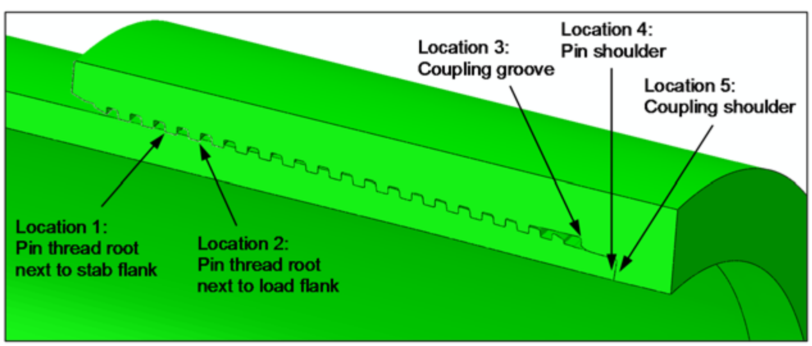

Figure 3. Critical locations for fatigue damage and structural failure within a premium casing connection.

3. Analysis of Casing Connection under Installation Loads

The first example is for casing installation in horizontal wells. Casing connections may be subjected to structural fatigue damage during installation and/or cementing operations. Horizontal wellbore designs often have a target curvature of 6°/100 ft to 20°/100 ft. The rotation of the casing strings during cementing operations within directional or horizontal wells will inherently give rise to fatigue loading conditions within the connections. This is due to the cyclic bending that occurs within the portion of the string positioned within the build section of such wells. As a result, the connections will experience different levels of strain variation (e.g. between axial tension and compression) which produces a severe elastic or plastic cyclic deformation.

Xie (2007) presented methodologies for analyzing casing connection under curvature loading. The connection can be modeled using axisymmetric solid elements with non-linear, asymmetric deformation. As noted in the Abaqus documentation (2013), these elements are intended for the non-linear analysis of structures which are initially axisymmetric, but which undergo non-linear, non-axisymmetric deformation. Contact between the pin and coupling elements was modeled using slide-lines.

As an example case, a generic 7 inch, 23 lb/ft L80 premium casing connection was analyzed under 12°/100 ft curvature loading following a nominal torque make-up. The generic connection model captured the basic features common to the premium connections currently used in shale gas well applications (e.g. buttress threads, torque shoulder, metal-metal radial seal) to ensure that the analysis produces results that are illustrative.

Figure 4 presents the axial strain distribution within the connection. The high compressive axial strains are represented in blue, while the high tensile axial strains are in red. The figure shows the significant variations that exist in the axial strain values at the same locations on the tension and compression sides of the connection. It is these variations in axial strain around the circumference that create the potential for fatigue damage during casing rotation.

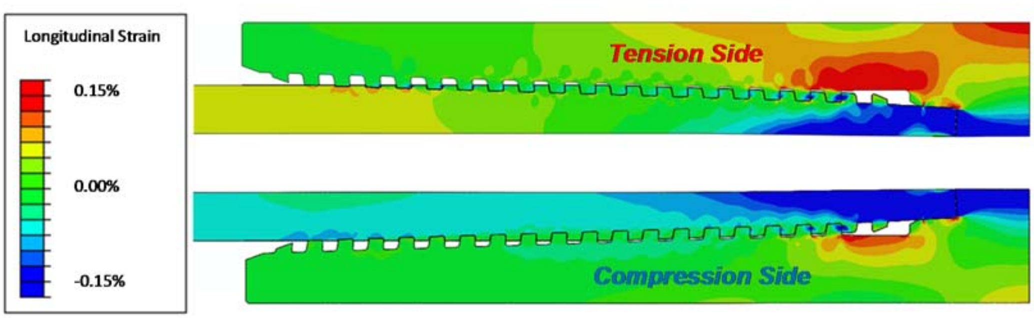

Figure 4. Longitudinal strain for a generic premium connection subjected to 12° /100 ft curvature loading.

Since the strain in the critical locations (e.g. as shown in Figure 3) may exceed the elastic limit, strain-based criteria should be used to assess the fatigue life of connections. Xie et al. (2011) proposed the use of several criteria, such as a modified Morrow approach (Dowling 1998), KBM approach (Kandil et al. 1982), and FS approach (Fatemi et al. 1988). The key features of these approaches are described in the following.

The modified Marrow approach takes the mean stress effect into account, and can be expressed in the following equation (Dowling 1998):

$$\bar{\varepsilon}_a = \frac{\sigma_f^{'} - \sigma_m^{'}}{E}(2N_f)^b + \varepsilon_f^{'}(2N_f)^c$$

where $\bar{\varepsilon}_a$ is the equivalent strain amplitude and $\sigma_m^{'}$ is the effective mean stress. According to this modified Morrow criteria, the effect of mean stress declines with increasing strain amplitude.

The KBM approach considers the effect of critical plane, and FS approach takes the normal stress on the critical plane into account. Equations for these two criteria can be found in Xie et al. (2011).

Based on analysis results as shown in Figure 4, the fatigue life predictions at the five critical locations (see Figure 3) derived using these respective criterion are presented in Figure 5 for the nominal make-up condition.

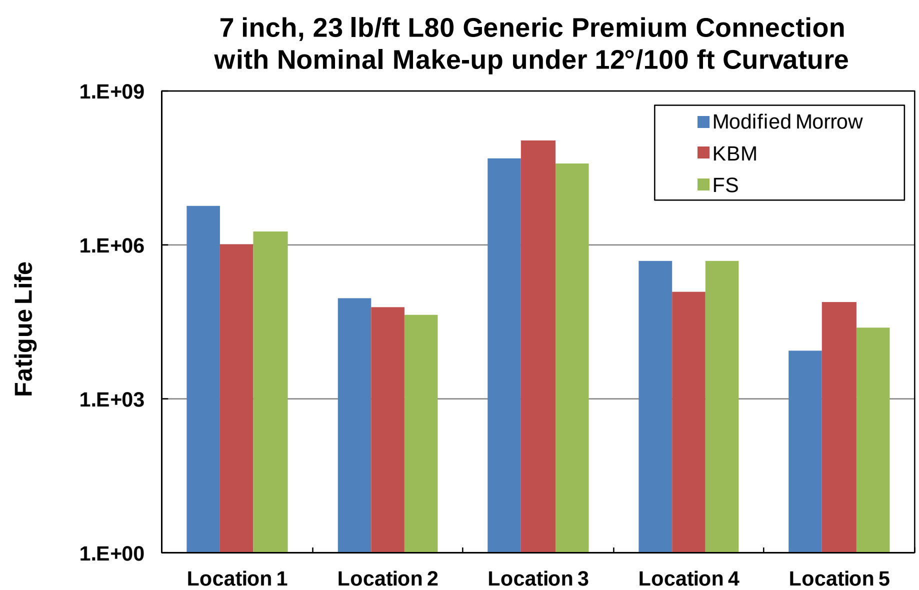

Figure 5. Fatigue life prediction for a generic premium connection with nominal make-up subjected to 12° /100 ft cyclic curvature loading.

As shown in Figure 5, Location 2 (i.e. thread root next to the load flank of the fourth pin thread from the coupling face) had a higher strain range and therefore a much lower fatigue life (i.e. as low as 4.4×10^4 based on the FS criteria). Location 5 (coupling shoulder region) also shows low fatigue life but the shoulder is not considered to be the primary failure location.

Typical well installation may have casing rotation at 20 RPM for 1.5 hours during cementing operations, giving a total of 1800 revolutions. The above analysis suggests that the generic premium connection should have fatigue life which is greater than the anticipated casing rotations during the installation for the horizontal well with the build section at 12°/100 ft.

4. Analysis of Casing under Stimulation Loads

The horizontal portion of the well is often completed with perforated casing. The perforations on the casing can be drilled prior to installation, or generated by perforating after installation.

Hydraulic fracturing may involve significantly high pressure in a short time period. According to Love (2005), injection pressure rates for hydraulic fracturing can reach up to 100 MPa (14.5 ksi) and 265 liters per second. During perforating, the explosion pulse pressure can be reached in a much short time period. Figure 6 shows the pressure pulses for perforating and hydraulic fracturing which are representative of shale gas wells.

The peak pressure during perforating or hydraulic fracturing is often much higher than the static yield pressure capacity of casing (e.g. 7.2 ksi for 7 inch, 23 lb/ft L80 casing). As such, dynamic FEA of the casing string should be used for perforating and hydraulic pressure loading. This allows for consideration of the effect of strain rate on material yield and tensile strengths.

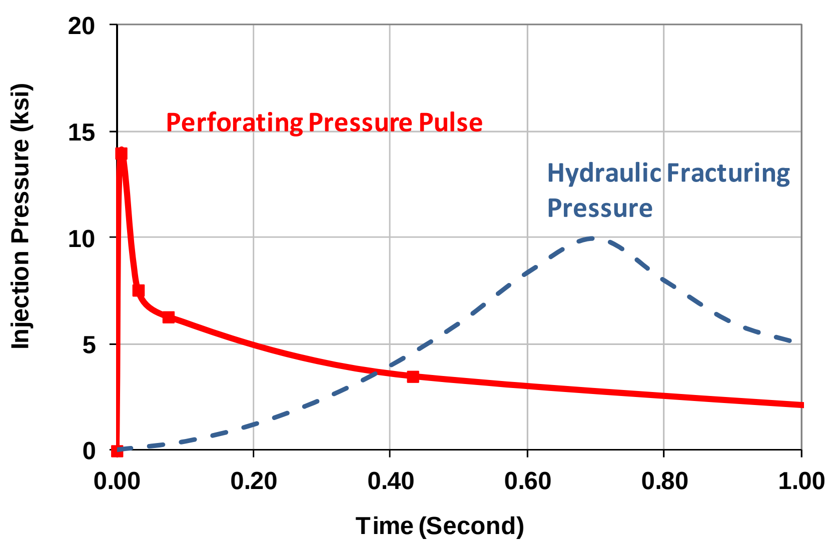

Figure 6. Assumed pressure pulses for perforating and hydraulic fracturing.

The effect of strain rate on the elastic-plastic response of the material can be considered using the following overstress power law (Ting 1961):

$$\dot{\bar{\varepsilon}}^{pl} = D\left(\frac{\bar{\sigma}}{\sigma_0} - 1\right)^p$$

in which $\dot{\bar{\varepsilon}}^{pl}$ is the equivalent plastic strain rate; $\bar{\sigma}$ is the yield stress at a non-zero plastic strain rate; σ_0 is the static yield stress; and D and p are material parameters defining the overstress power law, which were set as $D = 20$ and $p = 6$ based on the experimental results of mild steel by Manjoine (1944).

Abaqus provides the capability to model the above equation for strain-rate effect; described as the hardening dependencies with an overstress power law (Abaqus 2013).

The analysis example considers a 7 inch, 23 lb/ft L80 perforated casing. The perforation is defined by a shot density of 8 shots/ft, phase angle of 135°/45°, and perforation diameter of 20.3 mm. The perforated casing string is modeled using three-dimensional solid elements for an interval with a few rows of perforations. The perforation pattern is modeled in detail so that the localized stress and strain concentrations at individual perforations can be investigated. Three loading models are analyzed: a static pressure, a dynamic pressure with the loading rate similar to hydraulic fracturing, and a dynamic pressure with the loading rate similar to perforating. The analyses are performed with pressure loading increased monotonically until casing deformation is significant.

Figure 7 presents the analysis results of casing diameter enlargement due to applied pressures for the three analysis models. The response of diameter enlargement is basically similar for these three models prior to the static yield pressure (i.e. 7.2 ksi); however, beyond the static yield pressure, the static modeling shows rapid expansion of the casing diameter leading, eventually, to casing rupture. On the other hand, dynamic modeling with consideration of strain rate impact predicts much higher pressure loading capacities for hydraulic fracturing and perforating. The pressures corresponding to 0.1 inch diameter enlargement are 8.7, 11.3 and 16.0 ksi for the static, hydraulic fracturing and perforating pressures.

The diameter enlargement results in high tensile strain at the perforations. When considering the initiation of casing material fracture at the perforations, the tensile strain is significantly higher than the elastic limit, and therefore can be represented by the plastic strain. Figure 8 presents the maximum plastic strain values in the perforated casing for the three models analyzed. The distribution of residual plastic strain resulting from a static pressure of 8.0 ksi is also shown in Figure 8. The plastic strain is highly localized at the both sides of each perforation, indicating that the casing would likely split axially if the strain at the holes exceeds the tensile limit of the casing material. Assuming 10% as the strain limit for the casing material, the corresponding pressure values are 8.3, 10.6, and 14.8 ksi for the static, hydraulic fracturing and perforating pressures, respectively.

This example demonstrates that the dynamic analysis model, with consideration of strain rate on material yield and tensile strengths, should be used for the prediction of allowable pressures for hydraulic fracturing and perforating.

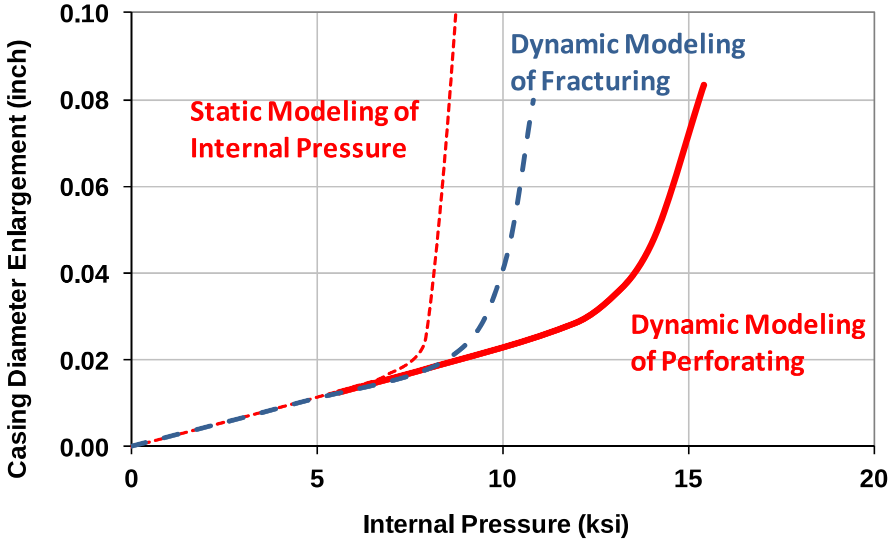

Figure 7. Casing diameter enlargement vs. internal pressure.

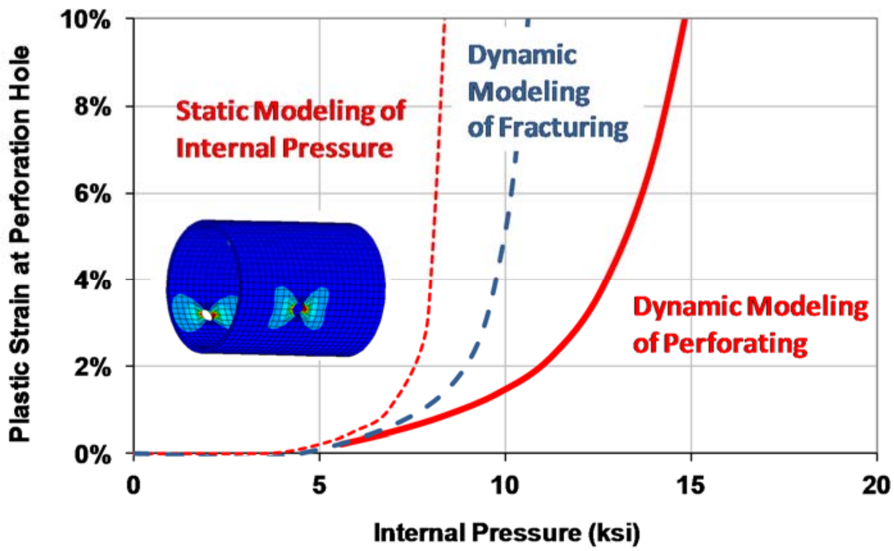

Figure 8. Plastic strain at perforation vs. internal pressure.

5. Analysis of Casing Connections under Shear Loads

Formation fractures resulting from the hydraulic fracturing process may inevitably cause formation movement. The formation shear movements refer to the opposite displacements about a plane which is angled with respect to the well axis. The formation shear movement is considered to be one of most severe loading scenarios in terms of structural integrity and sealability of casing connections (Xie et al. 2011).

One of the critical scenarios which must be examined is the leakage resistance of casing connections when they are positioned at the shear center plane, as shown on the left of Figure 9. On the right side of Figure 9 is a schematic representation of contact stress in the seal region which can be used to assess the sealability of a premium connection.

Published research papers have described empirical relationships for the sealability of premium tubular connections as a function of seal contact stress and seal length. In one such study, Murtagian et al. (2004) performed physical tests and numerical modeling to investigate the relationship between the sealability of stationary metal-to-metal seals and the seal contact profile, both with and without thread compounds. They proposed a weighted area of seal contact stress, W_a, as a means to evaluate the sealability of a connection, which was defined by:

$$W_a = \int_0^L P_c^n\,(l)\,dl$$

where $P_c(l)$ is the seal contact pressure, L is the seal length, and n is a correlation exponent. Based on test results, Murtagian et al. (2004) proposed values of 1.2 and 1.4 for the exponent n, for connections with and without sealing compounds, respectively.

A premium connection might be considered to provide acceptable seepage resistance when the weighted area of seal contact stress (W_a) was greater than some critical value W_{ac}:

$$W_a \geq W_{ac}$$

Based on review of the available data and the incorporation of the ISO 13679 leakage rate limit, Xie (2013) proposed the following equation for calculating the critical value of W_{ac} for tubular connections for stimulated applications (e.g. HPHT):

$$W_{ac} \;=\; 0.0022\,\left(\frac{P_{gas}}{P_{atm}}\right)^{0.838} \qquad (\text{ft}\cdot\text{ksi}^{1.4})$$

Assuming that the required containment pressure for the hydraulic fracturing application is 14.5 ksi, the critical value of W_{ac} would be 0.72 ft·ksi$^{1.4}$.

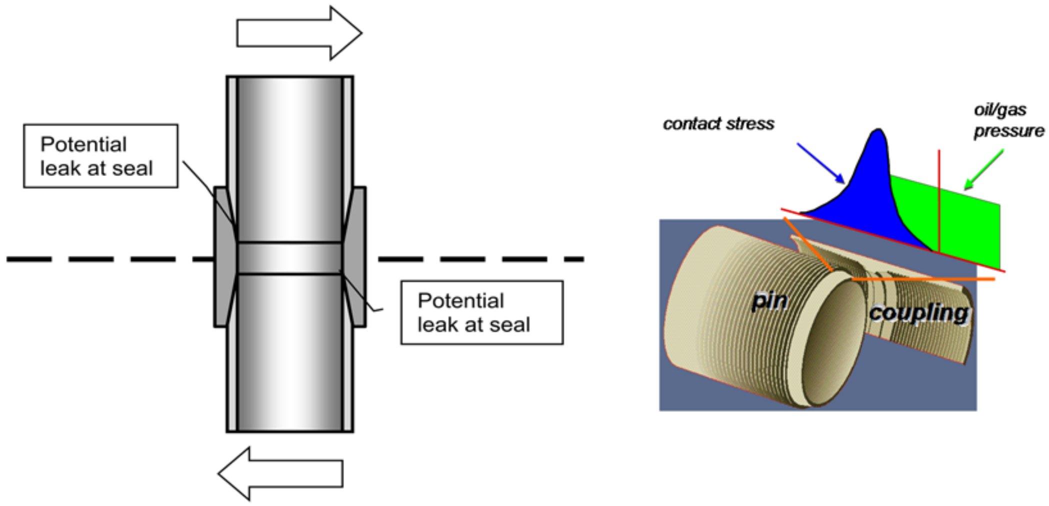

Figure 9. Schematic representation of connection model under shear (left) and contact stress distribution on the seal (right).

An example case with a 7 inch, 23 lb/ft L80 generic connection is presented here. The FEA of the impact of formation shear movement on connection sealing capacity is carried out in two steps. First, to determine the shear force to be applied to the connection model, analysis is performed with a casing string modeled as beam elements subjected to formation shear loading, where casing formation interaction is represented by a series of spring elements distributed along the axis of the model (Xie 2008). Note that the shear force determined here varies with the formation elastic modulus. In the second step, the shear force determined from the beam model is applied to a casing connection model constructed using axisymmetric-asymmetric solid elements. The connection model considers a relatively short interval with both ends clamped to allow the resultant bending moments to be generated. Shear forces are applied at both ends.

Figure 10 presents the analysis results of the weighted area of seal contact stress versus formation shear movement for the formation elastic modulus values of 300, 750, 1500, 2000 and 3000 ksi. As shown in the figure, the weighted area starts with 3.52 $ft \cdot ksi^{1.4}$ for all cases prior to the application of shear movement. The weighted area decreases with formation shear movement and formation elastic modulus. As the shear movement increases further, the weighted area of contact stress decreases below the sealing limit established for containing 14 ksi hydraulic fracturing pressure. The critical values of formation movements corresponding to the leakage limit are 0.108, 0.082, 0.067, 0.050 and 0.046 inch for the formation elastic modulus of 300, 750, 1500, 2000 and 3000 ksi, respectively.

This example demonstrates that the sealing capacity of a premium connection can decrease significantly under the formation shear movement. It should be considered a critical load case in the casing design for shale gas wells.

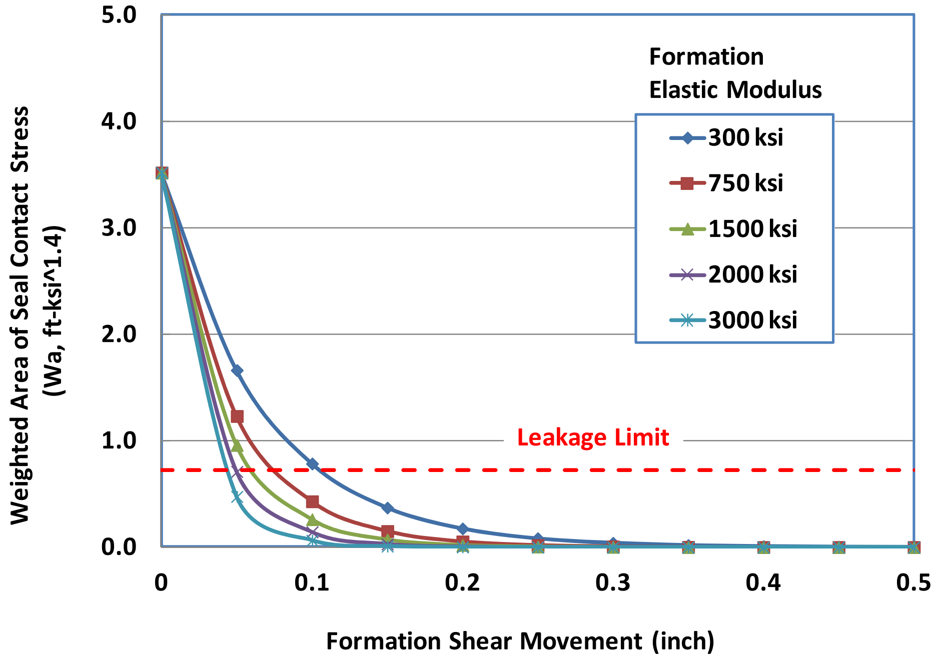

Figure 10. Analysis results of the weighted area of seal contact stress vs. formation shear movement.

6. Conclusions

This paper presents several considerations for FEA modeling of casing and casing connections for the shale gas well application. Based on the analysis of example cases, the following conclusions are made:

- A methodology is presented for assessing well fatigue life during installation (as the casing string is rotated over the build section) using FEA of casing connections under bending. The critical locations for connection fatigue failure are found to be in the thread roots near the coupling entry plane.
- The dynamic analysis model with consideration of strain rate on material yield and tensile strengths is presented for the prediction of allowable pressures for hydraulic fracturing and perforating.
- FEA of connection under formation shear loading shows that the sealing capacity of a premium connection can decrease significantly. The formation shear movement should be considered to be a critical load case in the casing design for shale gas wells.

7. References

1. Abaqus, “User Manual,” Version 6.13, 2013.
2. Dowling, N. E., “Mechanical Behavior of Materials – Engineering Methods for Deformation, Fracture, and Fatigue,” 2nd edition, Prentice Hall, New Jersey, 1998.
3. Fatemi, A. and Socie, D.F., “A Critical Plane Approach to Multi-axial Fatigue Damage Including Out-of-Phase Bending,” Fatigue and Fracture of Engineering Materials and Structures, 11, pp. 149-165, 1988.
4. Ghassemi, A., “A Geomechanical Analysis of Gas Shale Fracturing and Its Containment,” A Technology Status Report, Texas A&M University, March 2011.
5. Kandil, F.A., Brown, M.W. and Miller, K.J., “Biaxial Low Cycle Fatigue Fracture of 316 Stainless Steel at Elevated Temperature,” Met. Soc. London, 280, pp. 203-210, 1982.
6. Love, A. H., “Fracking: The Controversy Over its Safety for Environment,” Johnson Wright Inc. December 2005.
7. Manjoine, M. J., “Influence of Rate of Strain and Temperature on Yield Stresses of Mild Steel,” Journal of Applied Mechanics, 11, A-211. 1944.
8. Murtagian G R, Fanelli V, Villasante J. A, et al., “Sealability of Stationary Metal-to-Metal Seals,” Journal of Tribology, Vol. 126, No. 3.: 591. 2004.
9. Nikiforuk, A., “Shale Gas: How Often Do Fracked Wells Leak?” The Tyee, January 9, 2013.
10. Payne, M.L., Schwind, B.E., “A New International Standard for Casing/Tubing Connection Testing,” SPE/IADC 52846, Presented at the SPE/IADC Drilling Conference, Amsterdam, Holland, March 9-11, 1999.
11. Wittmeyer, H., “Fracking and Well Casing Failures,” Fracwire, June 27, 2013.
12. Xie, J., “Analysis of Oil Well Casing Connections Subjected to Non-axisymmetric Loads,” Abaqus Users’ Conference, Paris, France, May 22-24: 634–646. 2007.
13. Xie, J. and Liu, Y., “Analysis of Casing Deformation in Thermal Wells,” Abaqus Users’ Conference, RI. 2008.
14. Xie, J., Fan, C., Tao, G. and Matthews, C. M., “Impact of Casing Rotation on Premium Connection Service Life in Horizontal Thermal Wells,” World Heavy Oil Congress, Edmonton, Alberta, Canada, 2011.
15. Xie, J., “Numerical Evaluation of Tubular Connections for HPHT Applications,” Baosteel Conference, Shanghai, China, 2013.

8. Acknowledgement

The work presented in this paper was supported by C-FER Technologies, Canada. The author would like to sincerely acknowledge Dr. Nader Yoosef-Ghodsi, Senior Research Engineer, for his technical advice and assistance in reviewing this paper.